

INVESTIGATION ON DISSOLUTION PATTERN AND MATHEMATICAL MODELING OF DRUG RELEASE OF QUERCETIN BY COMPLEXATION WITH CYCLODEXTRIN NANOSPONGES

SOBITHARANI P^{1*}, ANANDAM S¹, MOHAN VARMA M², VIJAYA RATNA J³, SHAILAJA P³

¹Department of Vijaya College of Pharmacy, Hyderabad, Telangana, India. ²Department of Pharmaceutical Technology, Shri Vishnu College of Pharmacy, Bhimavaram, Andhra Pradesh, India. ³Department of Andhra University College of Pharmaceutical Sciences, Visakhapatnam, Andhra Pradesh, India. Email: sobhitarani@gmail.com

Received: 28 February 2019, Revised and Accepted: 10 April 2019

ABSTRACT

Objective: The main objective of this study was to investigate the release pattern of a poorly water-soluble drug quercetin (QU) by fabricating its cyclodextrin nanosponges.

Methods: Characterization of the original QU powder and QU-loaded nanosponges was carried out by the Fourier-transformed infrared (FTIR) spectroscopy, transmission electron microscopy (TEM), and dissolution tester. The drug release pattern was subjected to various kinetic models.

Results: FTIR studies confirmed the formation of inclusion complex of drug. The particle size analysis revealed that the average particle size measured by laser light scattering method is around 400–420 nm with low polydispersity index. The particle size distribution is unimodal and having a narrow range. A sufficiently high zeta potential indicates that the complexes would be stable and the tendency to agglomerate would be miniscule. TEM image revealed the porous nature of nanosponges. The dissolution of the QU nanosponges was significantly higher compared with the pure drug.

Conclusion: From the kinetic study, it is apparent that the regression coefficient value closer to unity in case of Korsmeyer-Peppas model indicates that the drug release exponentially to the elapsed time. *n* value obtained from the Korsmeyer-Peppas plots, i.e., 0.9911 indicating non-Fickian (anomalous) transport; thus, it projected that delivered its active ingredient by coupled diffusion and erosion.

Keywords: Nanosponges, Cyclodextrins, Complexation, Dissolution, Release kinetics, Quercetin.

© 2019 The Authors. Published by Innovare Academic Sciences Pvt Ltd. This is an open access article under the CC BY license (<http://creativecommons.org/licenses/by/4.0/>) DOI: <http://dx.doi.org/10.22159/ajpcr.2019.v12i5.32864>

INTRODUCTION

Flavonoids are a group of phenolic compounds that are widely distributed in different plant foods such as fruits, vegetables, leaves, and grains. There are different classes of flavonoids, for example, flavones, flavonones, isoflavones, flavonols, flavanonols, and anthocyanins [1,2]. Quercetin (QU) (3,3',4',5,7-pentahydroxyflavone) is an abundantly distributed plant; flavonol shows a wide range of pharmacological activities such as antioxidant, radical scavenging, and anticarcinogenic activity and is helpful in the recovery of *n*-diethyl nitrosamine-induced carcinogenesis [3,4], human leukemia cell [5], streptozotocin-induced diabetes [6], chronic renal failure, and reactive oxygen species-induced DNA damage [7]. QU and other flavonoids have been shown to modify eicosanoid biosynthesis, protect low-density lipoprotein from oxidation, prevent platelet aggregation, and promote relaxation of cardiovascular smooth muscle in antihypertensive and antiarrhythmic effects. In spite of this wide spectrum of pharmacological properties, its use in pharmaceutical field is limited by its low water solubility. QU is extremely hydrophobic in nature and has such poor absorption in the gastrointestinal tract. QU has a low solubility (7.7 µg/mL in water, 5.5 µg/mL in simulated gastric fluid, and 28.9 µg/mL in simulated intestinal fluid), which contributes to a low absorption *in vivo*. Its oral bioavailability is <17% in rats, even 1% in men [8-12]. As a result, the clinical application of the drug is greatly restricted. All these highlight the need for an improved formulation for QU with enhanced dissolution so that its absorption can be greatly enhanced. To overcome the above problems of QU and to achieve better clinical efficacy, many new drug delivery systems have been studied and developed in recent years, of which nanodrug delivery system has become a research hotspot with their numerous advantages such as reducing particle size, enhancing

surface area, increasing drug permeability, improving intracorporeal circulation and distribution of the drug, and enhancing drug targeting and so on [13].

Cyclodextrins (CDs) are cyclic oligosaccharides joined to each other by α -(1→4)-linkages and synthesized by the enzymatic degradation of hydrolyzed starch. They consist of both hydrophilic inclusion complexes with functional groups on lipophilic compounds in aqueous solution [14]. The use of CDs represents another novel technological approach to increase drug solubility, stability, and oral bioavailability [15,16]. However, the inclusion constants of native CDs rarely exceed the value of 10^3 . The cavity size of α -CD is insufficient for many drugs and γ -CD is expensive [17,18]. In general, β -CD has weaker complexing ability than conventional CDs. Among all CDs, β -CD is receiving attention due to its low cost and cavity size suitable for the widest range of drugs in aqueous media [19]. However, the low aqueous solubility and nephrotoxicity limited the use of β -CD, especially in parenteral drug delivery. Recently, CD-based nanosponges have emerged as a promising drug delivery platform for recalcitrant, difficult-to-formulate molecules [20-22].

Nanosponges are recently developed hypercross-linked CD polymers nanostructured to form three-dimensional networks; they are obtained by reacting CD with a suitable cross-linking agents. CD-based nanosponges showed superior complexing ability than natural CDs toward many molecules. They have been used to increase the solubility of poorly soluble actives, to protect the labile groups, and to control the release [23]. The present study was designed to investigate the feasibility of utilizing the CD-based nanosponges to improve the aqueous solubility and dissolution characteristics of QU.

MATERIALS AND METHODS

Materials

QU was purchased from Sigma-Aldrich, Singapore. CD nanosponges were prepared in our laboratory as reported elsewhere [24]. All other reagents used in the study were of reagent grade.

Methods

Preparation of QU-loaded nanosponges (QUNS)

Drug-loaded nanosponges were prepared by lyophilization technique as previously reported. Accurately weighed quantities of nanosponges were suspended in 50 mL of Milli-Q water using a magnetic stirrer, and then, the excess amount of QU was added and the mixture was sonicated for 10 min and was kept for 24 h under stirring. The suspensions were centrifuged at 2000 rpm for 10 min to separate the uncomplexed drug as a residue below the colloidal supernatant. The supernatant was lyophilized on a lyophilizer (LARK INDIA) at -20°C temperature and operating pressure 13.33 mbar. The dried powder was stored in a desiccator [25].

Determination of QU loading in NS

Weighed amount of QUNS complexes was dissolved in methanol, sonicated for 10 min to break the complex, diluted suitably, and then analyzed by ultraviolet (UV) spectrophotometer at 372 nm.

We used a previously reported formula to calculate "percent drug association:"

$$\frac{C' M' 100}{T' W}$$

Where, C is the concentration of QU measured in mg, M is the total particle mass – the yield of the formulation, T is the particle mass tested – weight of NS formulation used for quantification of QU, and W is the initial weight of the drug fed for loading – known amount of drug used for formulation.

Characterization of QU nanosponge complexes (QUNS)

The Fourier transformed infrared (FTIR) spectra of β -CD, plain nanosponges (NS2), QU, and QUNS complexes (QUNS2) were carried out by potassium bromide disk method using Tensor 27 FTIR spectrophotometer (Bruker Optics, Germany) in the region of $4000\text{--}600\text{ cm}^{-1}$. The particle size distribution was observed using a Mastersizer 2000 (Malvern Instruments Ltd., Worcestershire, UK) and the zeta potential of the same was determined using a Zetasizer (Malvern Instruments Ltd., Worcestershire, UK). The morphology of the QUNS was observed under transmission electron microscopy (TEM) (JEM-2000 EXII; JEOL, Tokyo, Japan).

Dissolution studies

The *in vitro* dissolution study of QU was carried out using multicompartiment ($n=6$) rotating cells with a dialysis membrane (Sartorius cutoff 12,000 Da). The donor phase consisted of formulations containing 5 mg of QU in 100 ml simulated gastric fluid (pH 6.4). The receptor phase also contains the same medium. The receptor phase was added with 0.5% w/v sodium lauryl sulfate (1 ml) to maintain proper sink conditions. The receptor phase was withdrawn completely after fixed time intervals, suitably diluted with distilled water and was analyzed using UV spectrophotometer at 372 nm. The experiment was carried out in triplicate.

Drug release kinetics

To elucidate the mode and mechanism of drug release, the data from the *in vitro* dissolution study were fitted into various mathematical models such as zero order, first order, Higuchi's, and Korsmeyer-Peppas model. The release data from the nanosponge formulation were determined by curve fitting method. Data obtained from *in vitro* release studies were fitted to various kinetic equations.

Zero-order model:

$$Q_t = Q_0 + K_0 t \quad (1)$$

Where, Q_t is the amount of drug dissolved in time t , Q_0 is the initial amount of drug in the solution, and K_0 is the zero-order release constant.

First-order model:

$$\ln(Q_{\infty} - Q_t) = \ln Q_0 + K_1 t \quad (2)$$

Where, Q_t is the amount of drug dissolved in time t , Q_0 is the initial amount of drug in the solution, Q_{∞} is the amount release in time ∞ (100% drug release), and K is the first-order release constant.

Higuchi model:

$$Q_t = k_H t^{1/2} \quad (3)$$

Where, Q_t is the amount of drug dissolved in time t and k_H is the Higuchi dissolution constant.

Korsmeyer-Peppas model (power law):

$$\frac{Q_t}{Q_{\infty}} = K K t^n \quad (4)$$

Or

$$\log Q_t = \log K_k + n \log t \quad (5)$$

Where, Q_t is the amount of drug dissolved in time t , Q_{∞} is the amount release in time ∞ , K_k is the rate constant, and n is the diffusional exponent, this indicates the drug release mechanism.

RESULTS AND DISCUSSION

Three types of β -CD nanosponges prepared by varying the cross-linking density were used in this study. QU was loaded into three types of nanosponges by lyophilization method. The drug loading was

Table 1: Percent drug loading in nanosponges

S. No.	Name of the formulation	Drug loading (%)
1	QUNS1	16 \pm 0.61
2	QUNS2	39 \pm 0.42
3	QUNS3	29 \pm 0.47

All determinations were performed in triplicate and values were expressed as mean \pm SD, $n=3$. SD: Standard deviation, QUNS: Quercetin-loaded nanosponges

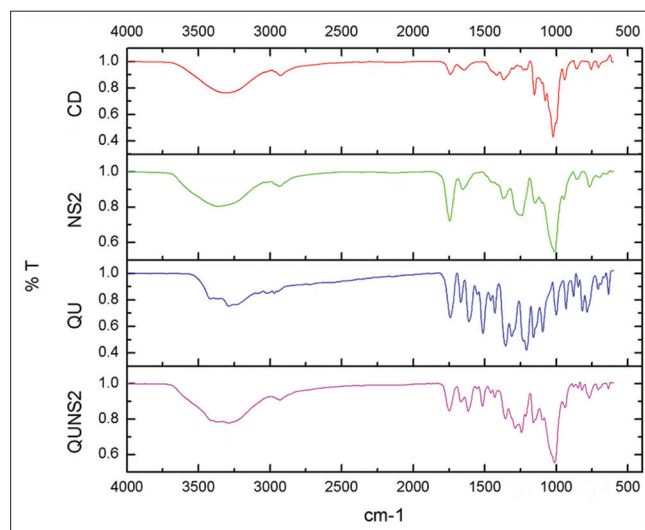


Fig. 1: Fourier transformed infrared spectra of β -cyclodextrin, plain nanosponges (NS2), quercetin (QU), and QUNS2

determined for the estimation of drug association with nanosponges, i.e., the amount of drug encapsulated into nanosponges, calculated by analyzing a fixed amount of formulation. Percent drug loading into all the three types of nanosponges (QUNS1-QUNS3) is presented in Table 1.

Among all the three types of nanosponges (NS1-NS3), the loading efficiency was found to be higher in NS2 (1:4 β-CD: DPC) as much as 39% w/w, while 16% and 29% w/w in NS1 and NS3 nanosponges, respectively. Due to the better solubilization and loading capacities, QUNS2 was selected for further studies.

FTIR spectroscopy

Fig. 1 shows a comparison of FTIR spectra of β-CD, NS2, QU, and QUNS2. NS2 showed a characteristic peak of carbonate bond at around 1720-1750 cm⁻¹ which confirms the formation of CD-based nanosponges. In addition, the other characteristics peak of NS was found at 2918 cm⁻¹ due to the C-H stretching vibration, 1418 cm⁻¹

due to C-H bending vibration, and 1026 cm⁻¹ due to C-O stretching vibration of primary alcohol. FTIR studies showed that there are weak interactions between NS and QU that were evident from broadenings and disappearance of the drug peaks in case of complexes. The comparison of FTIR spectra of QU and complex showed that there is a major change in the fingerprint region, i.e., 900-1400 cm⁻¹. The main characteristic peaks of QU are at around 1663, 1608, 1383, 1318, 1265, 1203, 1167, and 820-940 cm⁻¹. These QU characteristic peaks were broadened or shifted in the formulations suggesting definite interactions between QU and NS. FTIR spectroscopy confirmed the formation of inclusion complex of QU with nanosponges.

Particle size, polydispersity index, and zeta potential determination

The particle size analysis of NS2 and QUNS2 suspensions revealed that the average particle size measured by laser light scattering method is around 400-420 nm with low polydispersity index. The particle size distribution is unimodal and having a narrow range as seen in Table 2. A sufficiently high zeta potential indicates that the complexes would be stable and the tendency to agglomerate would be miniscule. A narrow PI means that the colloidal suspensions are homogenous in nature.

Table 2: Particle size and zeta potential of quercetin complexes

Sample	Mean hydrodynamic diameter±SD (nm)	Polydispersity index	Zeta potential (mV)
NS2	408±18	0.18±0.005	-19.34±1.8
QUNS2	413±27	0.25±0.005	-20.55±1.4

All determinations were performed in triplicate and values were expressed as mean±SD, n=3. SD: Standard deviation, QUNS: Quercetin-loaded nanosponges

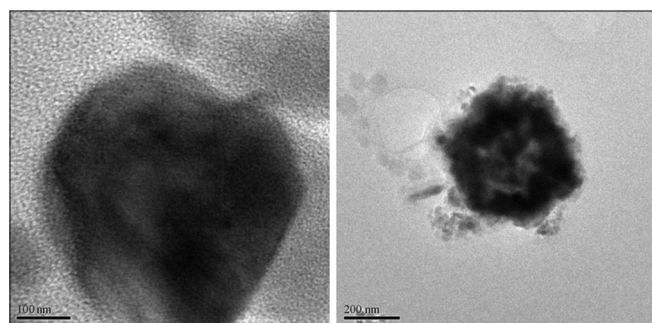


Fig. 2: Transmission electron microscopy images of plain nanosponge and quercetin-loaded nanosponges

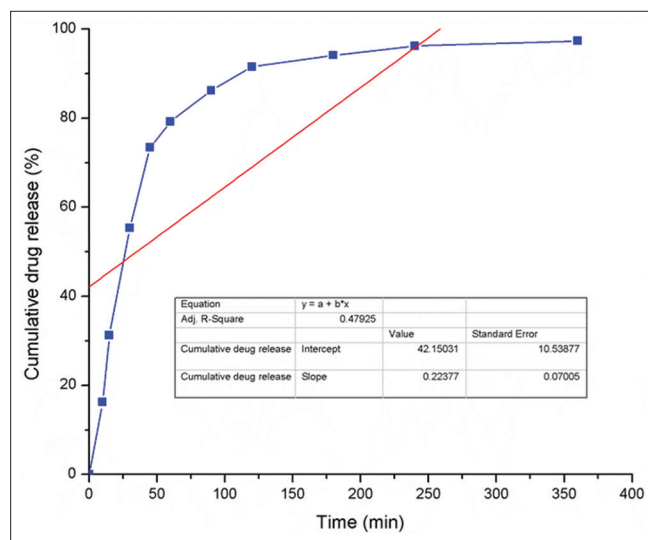


Fig. 4: Plot of zero-order release kinetics of the quercetin-loaded nanosponges formulation

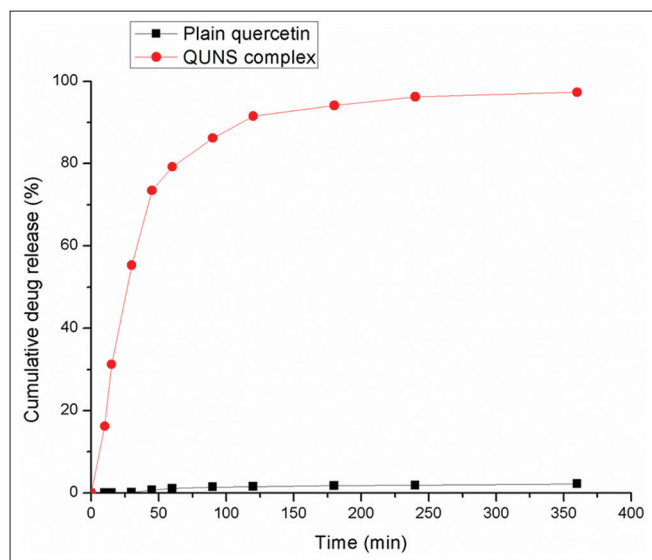


Fig. 3: Dissolution profile of original quercetin and quercetin-loaded nanosponges

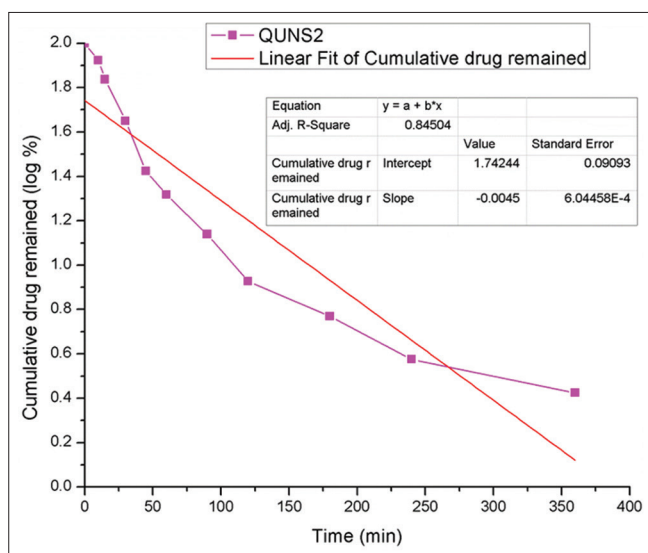


Fig. 5: Plot of first-order release kinetics of the quercetin-loaded nanosponges formulation

Table 3: Release kinetics of optimized formulation of quercetin nanosponge complex

Formulation code	Zero order		First order		Higuchi		Korsmeier-Peppas	
	R ²	n	R ²	n	R ²	n	R ²	n
QUNS	0.47925	0.22377	0.84504	0.0045	0.76092	5.41628	0.976	0.9911

QUNS: Quercetin-loaded nanosponges

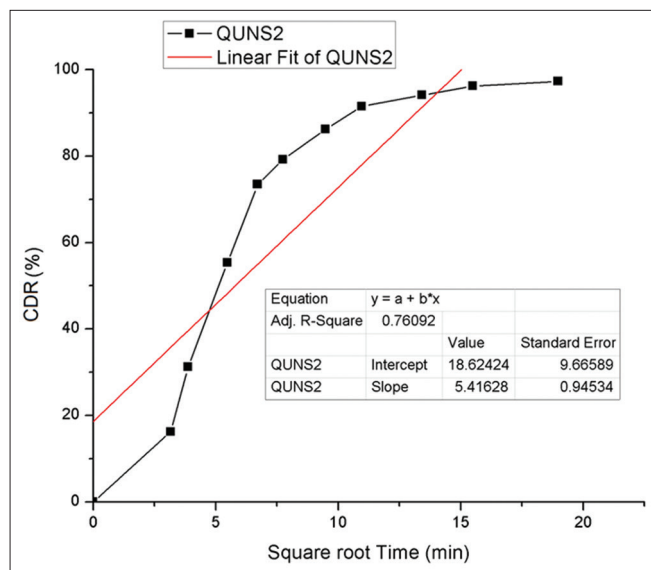


Fig. 6: Plot of Higuchi release kinetics of the quercetin-loaded nanosponges formulation

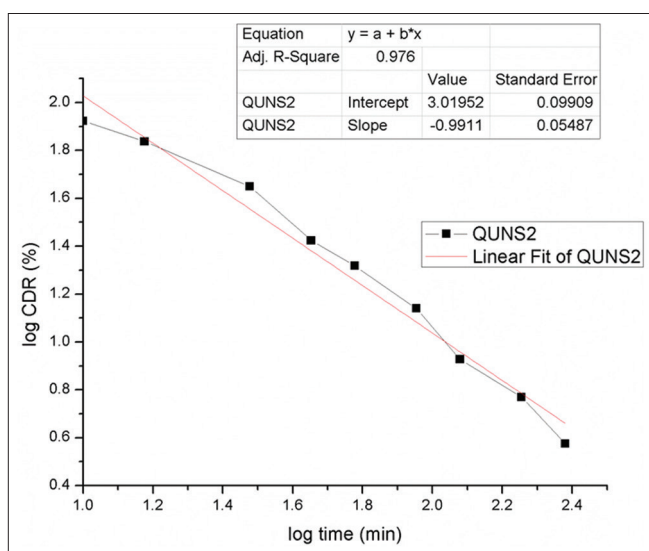


Fig 7: Plot of Korsmeier-Peppas release kinetics of the quercetin-loaded nanosponges formulation

TEM

TEM studies showed that the regular spherical shape and size of both the nanosponges that are unaffected even after drug encapsulation. TEM measurement revealed the porous structure of nanosponges as shown in Fig. 2. TEM studies revealed the porous structure of nanosponges and size of NS that are unaffected even after drug encapsulation (Table 3).

In vitro release of QU from nanosponge formulations

The dissolution profiles of plain QU and QUNS2 complex in simulated gastric medium are shown in Fig. 3. The *in vitro* release experiments showed a rapid and complete release of QU from nanosponges. From

in vitro release, it was found that the complex showed a significant improvement in the rate of release as compared with the pure drug. The dissolution of pure QU is not even 2% in 120 min, whereas the drug encapsulated in nanosponges showed faster release. An average 45–55% QU was released within 30 min showing rapid burst release. This was normally attributed to the fraction of QU which was adsorbed or encapsulated as non-inclusion complex on the NS surface. On the addition of the formulation to the release medium, this fraction of QU was diffused rapidly into the surrounding liquid. The maximum release of QU after 120 min from QUNS2 was 91.54%. After the initial effect, the release rate was found to be slower from the complex. The slower and sustained release of QU can be attributed to diffusion of the QU entrapped within the nanosponges as inclusion complex.

Release kinetics

Drug release data for the nanosponge formulation were fitted into various kinetic equations to find out the order and mechanism of drug release. The various release kinetic curves are shown in Fig. 4-7. The correlation coefficient showed that the release profile followed the Korsmeier-Peppas model ($R^2=0.976$), the release exponent, n was found to be 0.9911 indicating non-Fickian (anomalous) transport. Kinetic analysis of drug release profiles showed that the systems predominantly released nimodipine in a non-Fickian (anomalous) with a strong correlation coefficient ($R^2=0.94572$) of Korsmeier-Peppas model.

From the above results, it is apparent that the regression coefficient value closer to unity in case of Korsmeier-Peppas model indicates that the drug release exponentially to the elapsed time. The data indicate a more linearity when plotted by the first-order equation. Hence, it can be concluded that the major mechanism of drug release follows first-order kinetics. Further, the translation of the data from the dissolution studies suggested possibility of understanding the mechanism of drug release by configuring the data into various mathematical modelings such as Higuchi and Korsmeier-Peppas plots. Further, n value obtained from the Korsmeier-Peppas plots, i.e., 0.9911 indicating non-Fickian (anomalous) transport; thus, it projected that delivered its active ingredient by coupled diffusion and erosion.

CONCLUSION

CD nanosponges have attracted the attention of many scientists due to their enhancing solubility of poorly water-soluble drugs. They can incorporate a wide range of hydrophilic and lipophilic drug molecules and they have the ability to form inclusion and non-inclusion complexes. The higher solubilization potential of nanosponges can be attributed to the formation of inclusion complex with drug as well as entrapment in the matrix form. From *in vitro* release, it was found that the complex showed a significant improvement in the rate of release as compared with the pure drug. Further, the translation of the data from the dissolution studies suggested possibility of understanding the mechanism of drug release by configuring the data into various mathematical modelings such as Higuchi and Korsmeier-Peppas plots. Further, n value obtained from the Korsmeier-Peppas plots, i.e., 0.9911 indicating non-Fickian (anomalous) transport; thus, it projected that delivered its active ingredient by coupled diffusion and erosion.

ACKNOWLEDGMENTS

We would like to thank Prof. K. Venu Gopal Reddy (Director, CFRD, Osmania University) for assistance with FTIR analysis and Mr. Rajender (Centre for Nanoscience and Technology, JNTUH, HYD-85) for technical support with TEM.

AUTHORS' CONTRIBUTIONS

All the authors have contributed equally.

CONFLICTS OF INTEREST

Declared none.

REFERENCES

- Aluani D, Tzankova V, Yordanov Y, Zhelyazkova A, Georgieva E, Yoncheva K. Quercetin: An overview of biological effects and recent development of drug delivery systems. *Pharmacia* 2016;63:52-60.
- Cirillo G, Vittorio O, Hampel S, Iemma F, Parchi P, Cecchini M, et al. Quercetin nanocomposite as novel anticancer therapeutic: Improved efficiency and reduced toxicity. *Eur J Pharm Sci* 2013;49:359-65.
- Middleton E, Kandaswami C. The Impact of Plant Flavonoids on Mammalian Biology: Implications for Immunity, Inflammation and Cancer. London: Chapman and Hall; 1993.
- Sánchez-Pérez Y, Carrasco-Legleu C, García-Cuellar C, Pérez-Carreón J, Hernández-García S, Salcido-Neyoy M, et al. Oxidative stress in carcinogenesis. Correlation between lipid peroxidation and induction of preneoplastic lesions in rat hepatocarcinogenesis. *Cancer Lett* 2005;217:25-32.
- Chen J, Kang J, Da W, Ou Y. Combination with water-soluble antioxidants increases the anticancer activity of quercetin in human leukemia cells. *Pharmazie* 2004;59:859-63.
- Anjaneyulu M, Chopra K. Quercetin attenuates thermal hyperalgesia and cold allodynia in STZ-induced diabetic rats. *Ind J Exp Biol* 2004;42:766-9.
- Cemeli E, Schmid TE, Anderson D. Modulation by flavonoids of DNA damage induced by estrogen-like compounds. *Environ Mol Mutagen* 2004;44:420-6.
- Reinboth M, Wolfram S, Abraham G, Ungemach FR, Cermak R. Oral bioavailability of quercetin from different quercetin glycosides in dogs. *Br J Nutr* 2010;104:198-203.
- Graefe EU, Wittig J, Drewelow B, Riethling AK, Mueller S, Wukasch I, et al. Relative systemic availability of the flavonoids quercetin and rutin in humans. *Arch Pharm Pharm Med Chem* 1999;332:20.
- Shaji J, Iyer S. Novel double loaded quercetin liposomes: Evidence of superior therapeutic potency against CCl4 induced hepatotoxicity a comparative study. *Asian J Pharm Clin Res* 2012;5:104-8.
- Kumari A, Yadav SK, Pakade YB, Singh B, Yadav SC. Development of biodegradable nanoparticles for delivery of quercetin. *Colloids Surf B Biointerfaces* 2010;80:184-92.
- Dhawan S, Kapil R, Singh B. Formulation development and systematic optimization of solid lipid nanoparticles of quercetin for improved brain delivery. *J Pharm Pharmacol* 2011;63:342-51.
- Li SJ, Liao YF, Du Q. Research and application of quercetin-loaded nano drug delivery system. *Zhongguo Zhong Yao Za Zhi* 2018;43:1978-84.
- Lakshmi PK, Kumar MK, Aishwarya S, Shyamala B. Formulation and evaluation of ibuprofen topical gel: A novel approach for penetration enhancement. *Int J Appl Pharm* 2011;3:25-30.
- Anjana MN, Sreeja CN, Joseph J. An updated review of cyclodextrins—an enabling technology for challenging pharmaceutical formulations. *Int J Pharm Pharm Sci* 2013;5:54-8.
- Bipranch KT, Ravindra KZ, Kiran P, Ashis KN, Ranadhir C. Preparation and spectroscopic characterization of inclusion complex of 2-phenyl-4h-benzo[d][1,3]oxazin-4-one and β -cyclodextrin. *Int J Pharm Pharm Sci* 2014;6:176-9.
- Zheng Y, Chow AH. Production and characterization of a spray-dried hydroxypropyl-beta-cyclodextrin/quercetin complex. *Drug Dev Ind Pharm* 2009;35:727-34.
- Carlotti ME, Sapino S, Ugazio E, Caron G. On the complexation of quercetin with methyl-b-cyclodextrin: Photostability and antioxidant studies. *J Incl Phenom Macrocycl Chem* 2011;70:81-90.
- Challa R, Ahuja A, Ali J, Khar RK. Cyclodextrins in drug delivery: An updated review. *AAPS PharmSciTech* 2005;6:E329-57.
- Szejtli J. Cyclodextrin in drug formulations Part I. *Pharm Technol Int* 1991;3:15-22.
- Szente L, Szejtli J. Highly soluble cyclodextrin derivatives: Chemistry, properties, and trends in development. *Adv Drug Deliv Rev* 1999;36:17-28.
- Lala R, Thorat A, Gargote C. Current trends in b-cyclodextrin based drug delivery systems. *Int J Res Ayurveda Pharm* 2011;2:1520-6.
- Ansari KA, Vavia PR, Trotta F, Cavalli R. Cyclodextrin-based nanosponges for delivery of resveratrol: *In vitro* characterisation, stability, cytotoxicity and permeation study. *AAPS PharmSciTech* 2011;12:279-86.
- Swaminathan S, Pastero L, Serpe L, Trotta F, Vavia P, Aquilano D, et al. Cyclodextrin-based nanosponges encapsulating camptothecin: Physicochemical characterization, stability and cytotoxicity. *Eur J Pharm Biopharm* 2010;74:193-201.
- Cavalli R, Trotta F, Tumiatti W. Cyclodextrin-based nanosponges for drug delivery. *J Incl Phenom Macrocycl Chem* 2006;56:209-13.